



Research

An antenna array utilizing slotted conductive slab: inspired by metasurface and defected ground plane techniques for flexible electronics and sensors operating in the millimeter-wave and terahertz spectrum

Esraa Mousa Ali¹ · Mohammad Alibakhshikenari² · Bal S. Virdee³ · Lida Kouhalvandi⁴ · Patrizia Livreri⁵ · Francisco Falcone^{6,7}

Received: 2 September 2023 / Accepted: 2 November 2023

Published online: 18 November 2023

© The Author(s) 2023 [OPEN](#)

Abstract

This paper describes an innovative design of an antenna array that is metamaterial inspired using sub-wavelength slots and defected ground structure (DGS) for operation over millimeter-wave and terahertz (THz) spectrum. The proposed antenna array consists of a 2×4 array of conductive boxes on which are implemented rectangular slots. The presence of dielectric slots introduces resonant modes within the structure. These resonant modes result in enhancing the electromagnetic fields within the slots, which radiate energy into free space. The resonant frequencies and radiation patterns depend on the specific geometry of the slots and the dielectric properties. The antenna array is excited through a single microstrip line. The radiating elements in the array are interconnected to each other with a microstrip line. Unwanted mutual coupling between the radiating elements can degrade the performance of the antenna. This was mitigated by defecting the ground plane with rectangular slots. It is shown that this technique can enhance the array's reflection coefficient over a wider bandwidth. The array was constructed on polyimide substrate having dielectric constant of 3.5 and thickness of 20 μm . The design was modelled, and its performance verified using an industry standard electromagnetic package by CST Studio Suite. The proposed array antenna has dimensions of $20 \times 10 \text{ mm}^2$ and operates between 80 and 200 GHz for radiation gain better than 4 dBi and efficiency above 55%. The peak radiation gain and efficiency are 7.5 dBi and 75% at 91 GHz, respectively. The operational frequency range of the array corresponds to a fractional bandwidth of 85.71%.

Keywords Antenna array · Metasurface · Defected ground structure · Millimeter-wave · Terahertz 6G · Wireless communications

✉ Mohammad Alibakhshikenari, mohammad.alibakhshikenari@uc3m.es; ✉ Francisco Falcone, francisco.falcone@unavarra.es; Esraa Mousa Ali, esraa_ali@aaau.edu.jo; Bal S. Virdee, b.virdee@londonmet.ac.uk; Lida Kouhalvandi, lida.kouhalvandi@ieee.org; Patrizia Livreri, patrizia.livreri@unipa.it | ¹Faculty of Aviation Sciences, Amman Arab University, Amman 11953, Jordan. ²Department of Signal Theory and Communications, Universidad Carlos III de Madrid, 28911 Leganés, Madrid, Spain. ³Center for Communications Technology, School of Computing and Digital Media, London Metropolitan University, London, UK. ⁴Department of Electrical and Electronics Engineering, Dogus University, 34775 Istanbul, Turkey. ⁵Department of Engineering, University of Palermo, viale delle Scienze BLDG 9, IT 90128 Palermo, Sicily, Italy. ⁶Department of Electric, Electronic and Communication Engineering and the Institute of Smart Cities, Public University of Navarre, 31006 Pamplona, Spain. ⁷School of Engineering and Sciences, Tecnológico de Monterrey, 64849 Monterrey, Mexico.



SN Applied Sciences

(2023) 5:345

| <https://doi.org/10.1007/s42452-023-05570-x>

SN Applied Sciences
A **SPRINGER NATURE** journal

1 Introduction

Millimeter-wave (mm-Wave) and terahertz (THz) spectrums represent the new frontiers of wireless communications technology, expected to facilitate seamless interconnection between ultra-high-speed wired networks and personal wireless devices. This advancement will simplify the utilization of bandwidth-intensive applications, particularly in indoor and local access scenarios [1]. Several different THz antenna arrays have been investigated recently. The THz antenna array reported in [2] combines metasurface technology with artificial magnetic conductor (AMC) technology. The metasurface structure was implemented by constructing a periodic arrangement of dielectric unit-cells on a thin conductive layer on top of a dielectric substrate. The unit-cells were engineered to interact with the impinging electromagnetic waves in a specific way to modify the dispersion characteristics of surface. The AMC was implemented on a dielectric medium of a specific thickness. The 2×2 antenna array was constructed on a $35 \mu\text{m}$ thick silicon wafer. The array has an impedance bandwidth of 4.56% and reflection coefficient of $< -16 \text{ dB}$ over 300–314 GHz. In [3] the radiation element comprising the 2×1 Thz antenna array resembles a petal shaped structure. The array is fabricated on a polyimide substrate with a thickness of $10 \mu\text{m}$, a relative permittivity of 3.5, and has dimensions of $2.920 \times 1.055 \text{ mm}^2$. Simulation using CST Studio Suite[®] was used to verify the array's performance. The array is shown to have an impedance bandwidth of 0.63% and reflection coefficient of $< -23 \text{ dB}$ at 714 GHz. The THz patch antenna array reported in [4] consists of 11 patch elements that are interconnected to each other and printed on a single-layer high frequency laminate with a power distribution network realized by a hollow waveguide made from a copper block. The simulated results show that the subarray can achieve an impedance bandwidth of 37% for the reflection coefficient of $< -10 \text{ dB}$ over 150–205 GHz.

Metasurfaces, the two-dimensional counterparts of metamaterials, are artificially engineered to manipulate electromagnetic waves, exhibiting a negative refractive index not found in nature [5, 6]. This methodology has been applied to reduce the physical dimensions and enhance the specifications of microwave components such as antennas, filters, couplers, and mixers [7]. Their unique properties have enabled the development of novel applications, concepts, and devices [8, 9]. As a result, metasurfaces are now widely utilized in the design of antenna devices [10, 11]. Furthermore, the exceptional specifications of metasurfaces allow antenna designers to implement new antenna systems that are

unattainable using traditional techniques. Research indicates that metasurface-based antennas offer extended operational bandwidth and increased radiated power [12–15]. The primary advantages that make metasurfaces appealing for antenna design compared to conventional methods include (i) the implementation of more compact antennas, (ii) larger bandwidth, (iii) improved radiation properties, and (iv) the ability to model multi-band functionality.

The paper describes an innovative antenna array using metasurface-inspired techniques and defected ground structure (DGS) technology for operation across the mm-wave and THz spectrum. It is demonstrated that these proposed approaches can realize a high-performance antenna in a compact footprint area for various high-frequency wireless communications, including 6G. The array consists of closely spaced conductive radiating slabs that include sub-wavelength slots, exciting resonant modes within the structure, which in turn radiate energy into free space. The ground plane is perforated with rectangular slots to mitigate unwanted coupling between the radiating elements, resulting in improved array performance.

2 Design of the proposed antenna array

The Fig. 1 illustrates the proposed antenna array, which comprises a 2×4 matrix of rectangular conductive slabs loaded with sub-wavelength dielectric slots. These conductive radiating boxes draw inspiration from metasurface structures, where the multiple slots on each patch serve as sub-wavelength scatters. This feature distinguishes metasurfaces from traditional frequency-selective surfaces (FSS). A traditional FSS has individual elements (periodicity) which are of the order of the operating wavelength (generally $\lambda/2$). The matrix size was selected to achieve directional radiation. The antenna array is excited via a single microstrip line on one side, with the radiating elements interconnected by microstrip lines. The ground plane features rectangular slots, each positioned directly beneath a radiating element. These slots are designed to mitigate unwanted mutual coupling between the radiating elements, thereby improving the array's overall performance. For fabrication, we used a polyimide substrate with a dielectric constant (ϵ_r) of 3.5 and a thickness of 20 microns.

The antenna array's structural dimensions that are given in Table 1 were chosen for the array to operate across the 80 to 200 GHz range. CST Studio Suite[®], which is a high-performance 3D electromagnetic tool, was used to analyze and determine the antenna's optimum dimensions. CST Studio Suite[®] is a powerful industry standard tool that provides accurate and detailed analysis in a

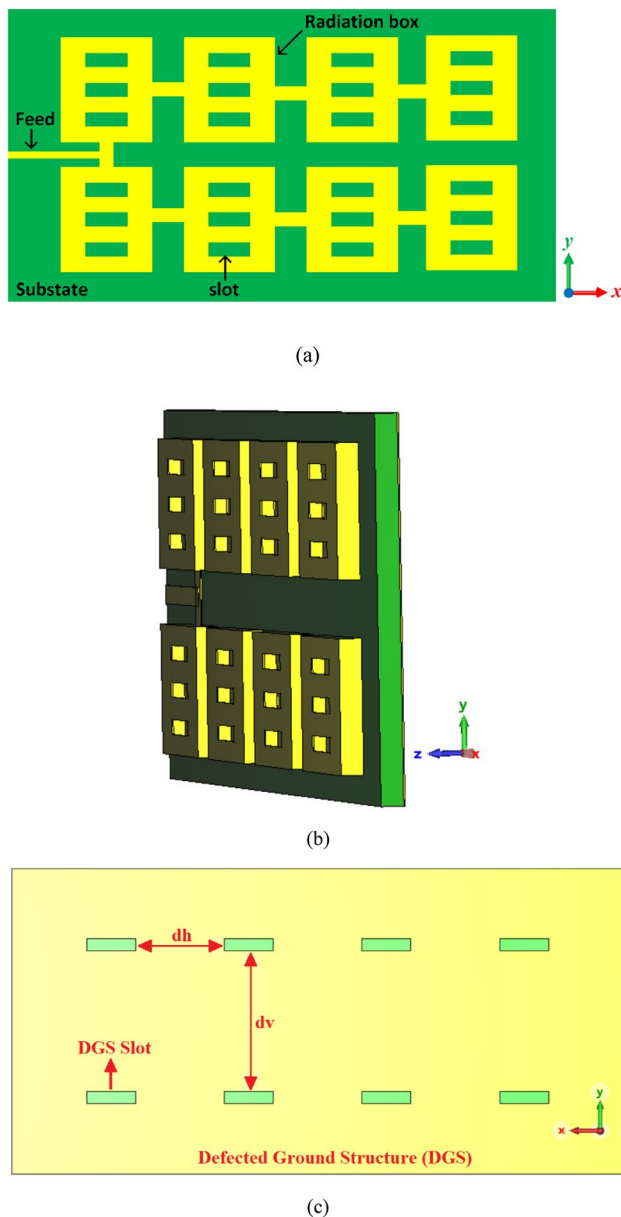


Fig. 1 Geometry and layout of the proposed 2×4 antenna array, (a) top view, (b) side view, and (c) back view

virtual environment, reducing the need for costly and time-consuming physical prototyping. Essentially slots are implemented on each of the conductive patches. The patch itself acts as a resonant structure. When properly designed, the dimensions of the patch and the dielectric substrate it's placed on determine its resonant frequency. This resonance causes a strong localized electric field at the patch edges and, therefore, the edges become the primary regions for radiation. Slots, or openings, that are introduced into the patch create breaks or discontinuities in the conducting surface of the patch. When electromagnetic waves from the feedline or incident from free space

interact with the slots, they couple energy into the microstrip structure. This interaction induces current flow on the conductive patch. The presence of the slots changes the current distribution on the patch compared to a solid patch. This non-uniform current distribution causes radiation from the antenna. Moreover, the electric field inside the slots interacts with the dielectric material, causing polarization of the dielectric. Depending on the frequency and dimensions of the slots, this polarization can lead to the generation of secondary currents within the slots. These slot currents act as sources of radiation, and they emit electromagnetic waves into free space.

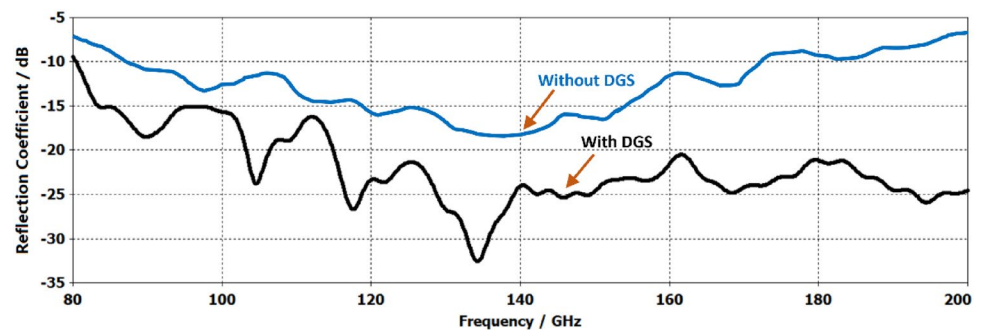
CST Studio Suite® was used to analyze the performance of the antenna array. This simulation tool is well-calibrated and validated against known measurement benchmarks, which is crucial in establishing the reliability of the simulated results presented here. The reflection coefficient of the proposed 2×4 antenna array is shown in Fig. 2. By defecting the ground plane, the impedance matching (for $|S_{11}| < -10$ dB) is improved and this is over a wider bandwidth. In the design of antenna arrays, as is the case here where the radiating elements are very closely spaced, mutual coupling between adjacent radiators can severely limit the array's bandwidth. This is because the mutual coupling causes energy from one antenna to interfere with the operation of neighboring antennas. By defecting the ground plane, the electromagnetic environment is altered resulting in reduction in the mutual coupling between the elements. As the results in Fig. 2 show the consequence of this is improved bandwidth performance of the array. The array operates over a very wide frequency range from 80 GHz to above 200 GHz for $|S_{11}| < -10$ dB, which corresponds to a fractional bandwidth of 85.71%.

The realized radiation gain and efficiency of the array are presented in Fig. 3. The gain exceeds 4 dBi, with efficiency consistently above 55% in the frequency range from 80 to 200 GHz. At its peak, the radiation gain reaches 7.5 dBi, while the efficiency reaches 75% at 91 GHz. Beyond 91 GHz, both the gain and efficiency decline. This is because the array was optimized at 91 GHz. At higher frequencies, this spacing between the radiating elements is longer be optimal, leading to reduced antenna array performance. A table summarizing the gain and efficiency at various frequencies within the 8 GHz to 200 GHz range is provided in Table 2.

The 2D radiation patterns of the proposed 2×4 antenna array is shown in Fig. 4 at various spot frequencies between 8 and 200 GHz. The antenna radiates energy essentially directionally, and the cross-polarization gain is more than 10 dB below the co-polarization over the 3 dB beamwidth. The good cross-polarization discrimination demonstrates that the array should reject signals with polarizations different from the desired polarization. This

Table 1 Antenna structural dimensions

Parameters	Size (mm)
Length of the antenna	20
Width of the antenna	10
Thickness of the antenna	0.6
Length of the horizontal interconnected lines (H shown in Fig. 1a)	1
Width of the horizontal interconnected lines (H shown in Fig. 1a)	0.4
Length of the vertical interconnected line (V shown in Fig. 1a)	1.5
Width of the vertical interconnected line (V shown in Fig. 1a)	0.5
Length of the feed line	3.25
Width of the feed line	0.5
Length of the radiation boxes	3.5
Width of the radiation boxes	3.5
Length of the metasurface slots	1.6
Width of the metasurface slots	0.4
Length of the ground plane	20
Width of the ground plane	10
Length of the DGS slots	1.6
Width of the DGS slots	0.4
Horizontal distance between DGS slots (d_h shown in Fig. 1c)	2.9
Vertical distance between DGS slots (d_v shown in Fig. 1c)	4.6

Fig. 2 Reflection coefficient of the proposed 2×4 array using metasurface-inspired techniques and DGS technology

rejection of cross-polarized signals should reduce interference. The radiation patterns show relatively low sidelobes.

3 State-of-the-art comparison

The proposed antenna array's characterizing parameters are compared with the state-of-the-art in Table 3. It is evident from the table that compared to the cited references the proposed antenna array design, which is metasurface-inspired and uses DGS technology, exhibits a much wider impedance bandwidth from 80 to 200 GHz and much higher average radiation efficiency of $\sim 65\%$. A wider bandwidth is advantageous, especially for mm-Wave and THz applications, where a broad operating frequency range is often desirable. These properties make this antenna suitable for existing and future mm-Wave and THz wireless systems.

4 Conclusion

A proof-of-concept is demonstrated for an innovative 2×4 antenna array designed for applications in the millimeter-wave and THz spectrum. The antenna array design draws inspiration from metasurface techniques and incorporates defected ground structure principles to enhance its radiation performance. The array consists of radiating elements comprising conductive slabs loaded with sub-wavelength slots. It is shown that the slots in the defected ground plane effectively mitigate unwanted mutual coupling between closely spaced radiating elements, thereby enhancing the impedance bandwidth of the array. The proposed antenna exhibits directional radiation between 80 and 200 GHz, with an average gain of approximately 5.5 dBi and a radiation efficiency of around 65%. The proposed antenna has dimensions of $20 \times 10 \times 0.6 \text{ mm}^3$.

Fig. 3 The gain and efficiency of the proposed antenna array, (a) realized gain and (b) radiation efficiency

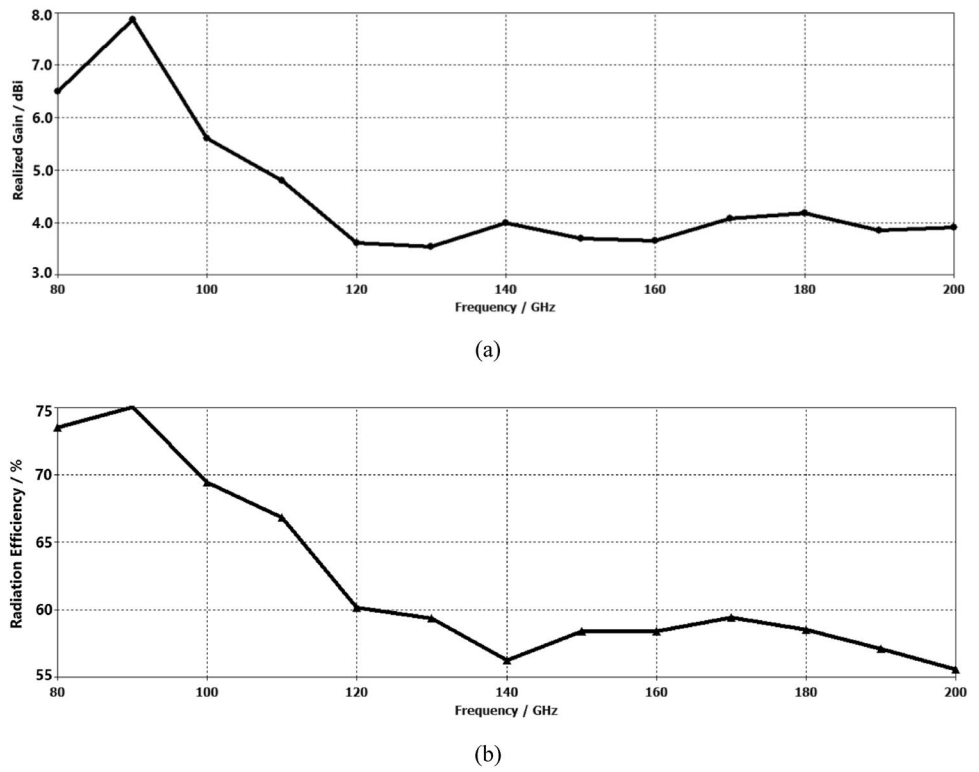


Table 2 Radiation properties

Freq. (GHz)	Radiation realized gain (dBi)	Radiation Eff. (%)
80	6.5	73.5
100	5.7	69
120	3.75	60
150	3.8	57
180	4.15	58
200	3.95	55.5

Fig. 4 Radiation patterns of the proposed 2×4 array slotted ground antenna at various spot frequencies, (a) 80 GHz, (b) 100 GHz (c) 120 GHz, (d) 150 GHz, (e) 180 GHz, and (f) 200 GHz

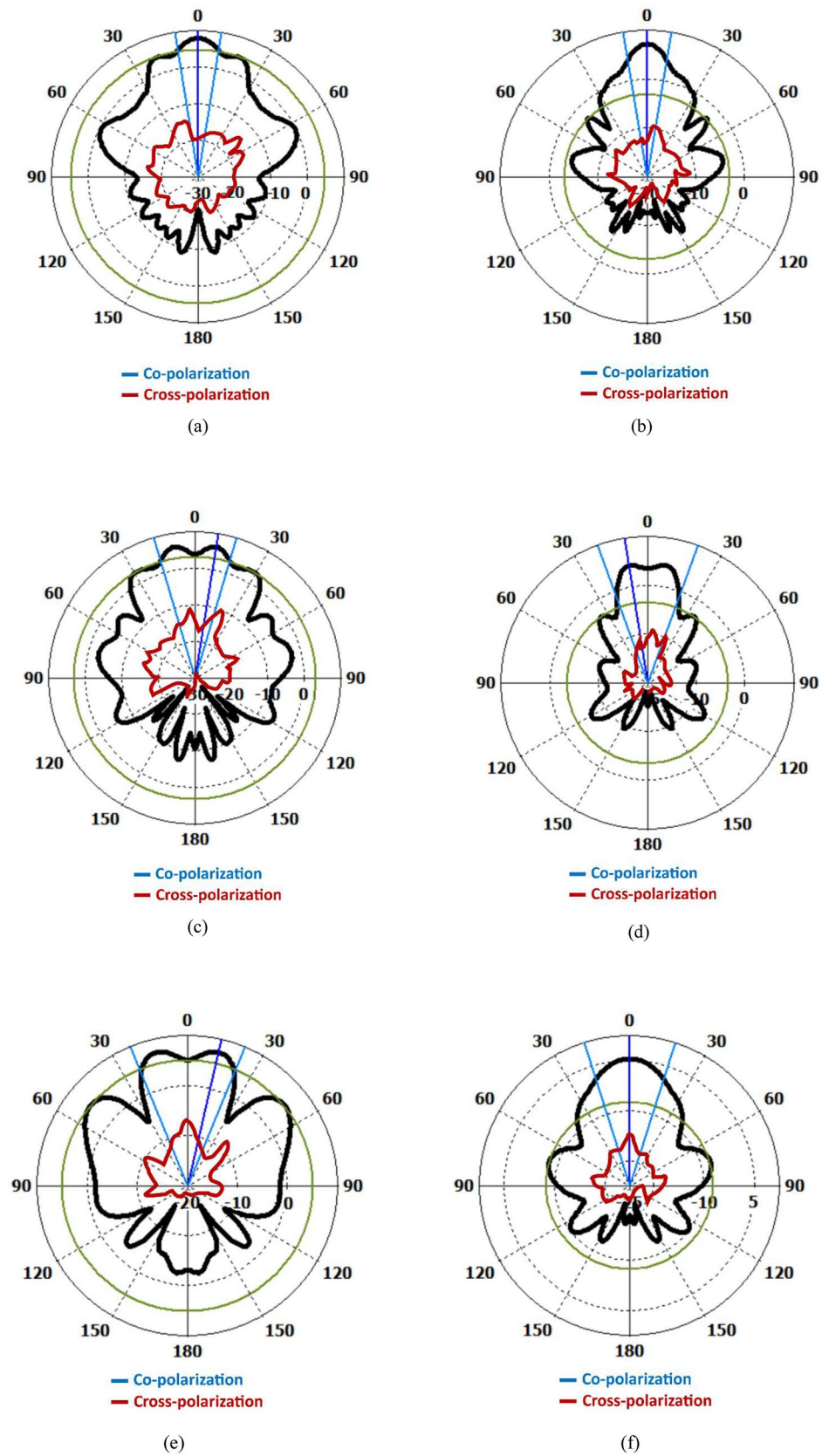


Table 3 Specification comparison of the proposed antenna with state-of-the-art

Ref	Antenna type	Freq. (GHz)	Gain (dBi)	Eff. (%)	Size (λ_0) ²	Design complexity
[16]	Half-mode cavity fed DRA	135	3.7	62	0.3×0.4	High
[16]	Half-mode cavity fed higher order mode DRA	135	6.2/7.5	46/42	0.3×0.4	High
[17]	Slot fed stacked DRA	130	4.7	43	0.8×0.9	High
[18]	DRA	135	2.7	43	0.8×0.9	High
[19]	Ring-shaped Monopole	50–70	≤ 0.02	≤ 35	0.2×0.22	Moderate
[20]	Circular Open-loop	57–67	≤ −4.4	–	0.16×0.18	Moderate
[21]	Bowtie-slot	90–105	≤ −1.78	–	0.71×0.31	High
[22]	Differential-fed Circularly Polarized	50–70	≤ −3.2	–	1.5×1.5	Moderate
[23]	Monopole	45–70	≤ 4.96	–	1.95×1.93	Moderate
[24]	Dipole-Antenna	95–102	≤ 4.8	–	–	High
This work	Metasurface and DGS	80–200	> 5.5	> 65	5.3×2.6	Low

Acknowledgements Dr. Mohammad Alibakhshikenari acknowledges support from the CONEX-Plus programme funded by Universidad Carlos III de Madrid and the European Union's Horizon 2020 research and innovation programme under the Marie Skłodowska-Curie grant agreement No. 801538. Besides above, this work was supported by Ministerio de Ciencia, Innovación y Universidades, Gobierno de España (Agencia Estatal de Investigación, Fondo Europeo de Desarrollo Regional -FEDER-, European Union) under the research grant PID2021-127409OB-C31 CONDOR.

Author contributions Conceptualization, E.M.A., M.A., B.S.V., L.K., P.L., F.F.; methodology, E.M.A., M.A., B.S.V., L.K., P.L., F.F.; software, E.M.A., M.A., B.S.V.; validation, E.M.A., M.A., B.S.V., L.K., P.L., F.F.; formal analysis, E.M.A., M.A., B.S.V., L.K., P.L., F.F.; investigation, E.M.A., M.A., B.S.V., L.K., P.L., F.F.; resources, E.M.A., M.A., B.S.V., L.K., P.L., F.F.; data curation, E.M.A., M.A., B.S.V., L.K., P.L., F.F.; writing—original draft preparation, E.M.A., M.A.; writing—review and editing, E.M.A., M.A., B.S.V., L.K., P.L., F.F.; visualization, E.M.A., M.A., B.S.V., L.K., P.L., F.F.; supervision, M.A., B.S.V., P.L., F.F.; project administration, M.A., B.S.V., P.L., F.F.; funding acquisition, M.A., F.F. All authors have read and agreed to the published version of the manuscript."

Funding Open Access funding provided by Universidad Pública de Navarra.

Data availability All data are included within the manuscript.

Declarations

Conflict of interest The authors declare no conflict of interest.

Open Access This article is licensed under a Creative Commons Attribution 4.0 International License, which permits use, sharing, adaptation, distribution and reproduction in any medium or format, as long as you give appropriate credit to the original author(s) and the source, provide a link to the Creative Commons licence, and indicate if changes were made. The images or other third party material in this article are included in the article's Creative Commons licence, unless indicated otherwise in a credit line to the material. If material is not included in the article's Creative Commons licence and your intended use is not permitted by statutory regulation or exceeds the permitted use, you will need to obtain permission directly from the copyright

holder. To view a copy of this licence, visit <http://creativecommons.org/licenses/by/4.0/>.

References

- Pietrenko-Dabrowska A et al (2022) A comprehensive survey on antennas on-chip based on metamaterial, metasurface, and substrate integrated waveguide principles for millimeter-waves and terahertz integrated circuits and systems. *IEEE Access* 10:3668–3692
- Alibakhshikenari M et al (2023) On-Chip Terahertz antenna array based on amalgamation of metasurface-inspired and artificial magnetic conductor technologies for next generation of wireless electronic devices. *AEU-Int J Electron C* 167(154684):1–14
- Shihzad W et al (2022) Design and analysis of dual-band high-gain THz antenna array for THz space applications. *Appl Sci* 12(921):1–20
- Sun G-H, Wong H (2023) A hollow-waveguide-fed planar wide-band patch antenna array for terahertz communications. *IEEE Trans Thtz Sci Technol* 13(1):10–19
- Sindreu MD et al. (2013) Composite right-/left-handed transmission line metamaterials In: *Wiley Encyclopedia of electrical and electronics engineering*. Wiley, Hoboken, pp 1–25. <https://doi.org/10.1002/047134608X.W8195>.
- Anthony L, Christophe C, and Tatsuo I (2004) Composite right/left-hand transmission line metamaterials. *IEEE microwave magazine*, vol 5(3), pp 34–50.
- Oliveri G, Werner DH, Massa A (2015) Reconfigurable electromagnetics through metamaterials— a review. *Proc IEEE* 103:1034–1056
- Caloz C, Itoh T (2005) *Electromagnetic metamaterials: transmission line theory and microwave applications*. Wiley, New Jersey, p 376. <https://doi.org/10.1002/0471754323>.
- Engheta N, Ziolkowski RW (2006) *Metamaterials physics and engineering explorations*. New IEEE Press, New Jersey, p 440. <https://doi.org/10.1002/0471784192>.
- Azpilicuetta L et al (2020) A comprehensive survey of "Metamaterial transmission-line based antennas: design, challenges, and applications. *IEEE Access* 8:144778–144808. <https://doi.org/10.1109/ACCESS.2020.3013698>

11. Aïssa S et al (2020) A comprehensive survey on various decoupling mechanisms with focus on metamaterial and metasurface principles applicable to SAR and MIMO antenna systems. *IEEE Access* 8:192965–193004. <https://doi.org/10.1109/ACCESS.2020.3032826>
12. Alici KB, Özbay E (2007) Radiation properties of a split ring resonator and monopole composite. *Phys Status Solidi B* 244:1192–1196. <https://doi.org/10.1002/pssb.200674505>
13. Siddiqui OF, Mo M, Eleftheriades GV (2003) Periodically loaded transmission line with effective negative refractive index and negative group velocity. *IEEE Trans Antennas Propag* 51:2619–2625
14. Keshwala U, Rawat S and Ray K (2019) Honeycomb shaped fractal antenna with defected ground structure for UWB applications. In: 2019 6th international conference on signal processing and integrated networks (SPIN). Noida, India, pp. 341–345. <https://doi.org/10.1109/SPIN.2019.8711752>.
15. Sandeep T, Tanushri M, Prashant B, Sanyog R, Kanad R (2017) Design and analysis of fabricated rectangular microstrip antenna with defected ground structure for UWB applications In: *Soft computing: Theories and applications*, Part of the advances in intelligent systems and computing book series, vol 584. AISC, pp 373–378. https://doi.org/10.1007/978-981-10-5699-4_34.
16. Hou D et al (2014) D-band on-chip higher-order-mode dielectric-resonator antennas fed by half-mode cavity in CMOS technology. *IEEE Antennas Propag Mag* 56(3):80–89
17. Hou D et al (2012) 130-GHz on-chip meander slot antennas with stacked dielectric resonators in standard CMOS technology. *IEEE Trans Antennas Propag* 60(9):4102–4109
18. Hou D et al. (2011) Silicon based on-chip antenna design for millimeter-wave/THz applications. EDAPS. Hanzhou, China, pp 1–4
19. Huang HT et al. (2015) A circular ring-shape monopole on-chip antenna with artificial magnetic conductor. APMC, Nanjing, China, pp 1–3
20. Bao XY et al (2012) 60-GHz AMC-based circularly polarized on-chip antenna using standard 0.18- μm CMOS technology. *IEEE Trans Ant Prop* 60(5):2234–2241
21. Khan MS, Tahir FA, Cheema HM (2016) Design of bowtie-slot on-chip antenna backed with E-shaped FSS at 94 GHz. 10th EuCAP. Davos, Switzerland, pp 1–3
22. Wang L, Sun W (2015) A 60-GHz differential-fed circularly polarized on-chip antenna based on 0.18- μm COMS technology with AMC structure. IET International Radar Conference, pp 1–4
23. Upadhyay S, Srivastava S (2013) A 60-GHz on-chip monopole antenna using silicon technology. AEMC, pp 1–2
24. Nafe M, Syed A, Shamim A (2015) Gain enhancement of low profile on-chip dipole antenna via artificial magnetic conductor at 94 GHz. 9th EuCAP, Lisbon, pp 1–3

Publisher's Note Springer Nature remains neutral with regard to jurisdictional claims in published maps and institutional affiliations.